Electronic and Molecular Structure of Aminimides (1-Acyl-2,2,2-trimethyldiazan-2-ium-1-ide). 1. Formaminimide ($HCON^-N^+Me_3$)†

Mircea D. Gheorghiu,* Ana Racoveanu,‡ and Mitchell R. Zakin*,‡

Department of Chemistry, Massachusetts Institute of Technology, Cambridge, Massachusetts 02139, and Physical Sciences Inc., Andover, Massachusetts 01810

Received: September 28, 2005; In Final Form: January 26, 2006

The electronic structure and geometries of (*Z*)- and (*E*)-H-$CON^-N^+(CH_3)_3$ have been examined at two levels of theory: B3LYP (basis sets 6-311+G(d,p), 6-311++G(d,p), and 6-311G(3df,3pd)) and MP2(full)/6-311++G(d,p). The (*Z*) conformation about the C(O)−N^- bond is thermodynamically preferred over the (*E*) configuration. Natural bond orbital calculation locates one lone pair of the N^- in the HOMO, which is the p_z natural hybrid orbital (perpendicular to the O═CN^-N^+ plane). The second lone pair (of lower energy) of N^- occupies the HOMO-3, which is the natural hybrid orbital $sp^{1.12}$ ($sp^{1.01}$ for the (*E*) conformation, $sp^{1.74}$ in the rotational transition state). The carbonyl π bond is the HOMO-2. The charge-transfer ability of the negative nitrogen in H-$CON^-N^+(CH_3)_3$ is more powerful than that of the neutral amidic nitrogen in dimethylformamide. The following facts convincingly sustain this view: (1) the higher rotational barrier (stronger C−N^- bond) in the case of H−$CON^-N^+(CH_3)_3$, (2) natural resonance theory analysis predicts almost equal weights for the (*Z*)-H−C(═O)$N^-N^+(CH_3)_3$ and the (*Z*)-H−$C(O^-)$═$NN^+(CH_3)_3$ canonical resonance structures whereas the weight of the $HCON(CH_3)_2$ structure is almost twice as large as that of $HC(O^-)$═$N^+(CH_3)_2$, and (3) the second-order perturbation stabilization, as a result of the donor (N^-)/acceptor (carbonyl) interaction, is 101.3 kcal/mol for H−$CON^-N^+(CH_3)_3$ and only 64.4 kcal/mol for dimethylformamide.

Introduction

Aminimides consist of an ylide group (N^-N^+) in which the electron-rich (negative) nitrogen is attached to a carbonyl function, a very good electron acceptor. Classic examples are the 1-acyl-2,2,2-trisubstituted diazan-2-ium-1-ides,[1,2] R-$CON^-N^+R_1R_2R_3$, which were discovered in 1959.[3] Despite this long history, the electronic properties of the $-CON^-N^+$ functionality remain largely unexplored, although a few recent studies have provided some insight. For example, the ylide segment $-N^-N^+(CH_3)_3$ is claimed to be the strongest electron donor among the uncharged organic substituents.[4] Therefore, one might expect, for example, that the insertion of the CON^-N^+ functionality in an appropriate position within a polyamide chain would strengthen the hydrogen bonding even more than an amide functionality. Indeed, a R-$CON^-N^+R_1R_2R_3$ tetrapeptide isostere scaffold was found to be a more potent inhibitor of HIV-1 protease than the parent peptide.[5]

It may seem surprising that in aminimides the sequence $-N^-N^+R_1R_2R_3$ "survives" and does not collapse (spontaneously?) to yield the more thermodynamically stable neutral hydrazine derivative $-NR_1NR_2R_3$. In fact the conversion of $-N^-N^+R_1R_2R_3$ into $-NR_1NR_2R_3$ only occurs at high temperature, close to the melting point of the respective compound. This rearrangement reaction of aminimides, known also as the Wawzonek rearrangement,[6] has only been observed when R_1 is an allyl or benzyl group. Although the Wawzonek rearrangement is an interesting phenomenon per se, we will examine this topic in a future contribution.

In amides and R-$CON^-N^+R_1R_2R_3$ the nitrogen lone pair is π-delocalized over the adjacent CO group. Intuitively, one expects charge delocalization in R-$CON^-N^+(CH_3)_3$ to be stronger than in amides since charge transfer is easier from a negatively charged species (in this case the negative nitrogen) than from a neutral atom (nitrogen from an amide function). Consequently, the oxygen atom (from the CO group in R-$CON^-N^+(CH_3)_3$) becomes a much better hydrogen bond acceptor than the amidic oxygen. Indeed, the hydrogen bond basicity of oxygen in benzoyl-2,2,2-trimethyldiazan-2-ium-1-ide (C_6H_5-$CON^-N^+(CH_3)_3$) is larger than that of the oxygen in *N*,*N*-dimethylbenzamide, (C_6H_5-$CON(CH_3)_2$).[4] Additionally, the ylide structure of R$CON^-N^+R_1R_2R_3$ provides an intrinsic large dipole moment, which would ensure stronger interaction with polar compounds or polar substructure. Therefore, it is not surprising that aminimides have been studied as pharmacophores and nonlinear optical materials.[4] Furthermore, the aminimide class R-$CON^-N^+R_1R_2R_3$ can also control the growth of plants,[7] and have antimicrobial,[8−11] vasodilation,[12] and diuretic and antihypertensive[13] effects. Aminimides have been successfully tested as carrier molecules for uphill transport through liquid membranes, as a model for assisted transport across the cell membrane.[14] Additionally, aminimides have become of interest to polymer chemists[15−24] as monomer or as isocyanate precursors.

Although aminimides are formally related to amides, the latter have been much more extensively studied. Because of its paramount importance in understanding the conformation of proteins, there has been a wealth of computational studies regarding the amide linkage.[25] This is in sharp contrast to the few computational and experimental studies devoted to R-$CON^-N^+R_1R_2R_3$ which have been concerned mostly with charge calculations at the AM1,[26] PM3,[27] and ab initio Hartree−

* To whom correspondence should be addressed. E-mail: M.D.G. mircea@mit.edu, M.R.Z. zakin@psicorp.com

† This paper is dedicated with gratitude to Professor Lawrence T. Scott on the occasion of his 60th birthday.

‡ Physical Sciences, Inc.

10.1021/jp055528a CCC: $33.50
Published on Web 03/02/2006

Fock levels of theory (basis sets Gaussian 4-31G, 6-31G*, 6-31G**).[4] A related ylide,[28] NO_2-$N^-N^+(CH_3)_3$, has been subjected to low-temperature high-resolution X-ray diffraction measurements and the experimental charge density topological properties have been examined in terms of Bader's atoms in molecule (AIM) concepts.[29]

To fill the knowledge gap for the properties of R-CON^-N^+-$R_1R_2R_3$, we have embarked on a more comprehensive analysis by means of density functional theory (DFT) and Møller−Pleset second-order perturbation theory (MP2) of the electronic and molecular structure aspects of model compounds R-CON^-N^+-$(CH_3)_3$. Our findings regarding H-$CON^-N^+(CH_3)_3$ are reported here (Part I), while the substituent effects (R-$CON^-N^+(CH_3)_3$) will be examined in a future submission.

Computational Details

All calculations were carried out with Gaussian 98[30] and 03[31] codes. Geometries of all structures were fully optimized at two levels of theory, namely Density Functional Theory[32,33] and Møller−Pleset[34] second-order perturbation theory, MP2(full). The density functional calculations employed the popular[35,36] hybrid functional B3LYP. It consists of the three-parameter hybrid exchange functional of Becke[37] and the nonlocal gradient-corrected correlation functional of Lee, Yang, and Parr.[38] Stationary points have been characterized by harmonic frequency analysis as local minima (no imaginary frequency) or first-order saddle point (one imaginary frequency). The computed rotational transition states (RTS) gave only a single imaginary frequency which when animated has the valid motion. Since H-CON^-N^+-$(CH_3)_3$ possesses several lone pairs of electrons to examine it inclusion of diffuse functions in the basis set is obligatory,[39,40] while weak contacts such as hydrogen bonding are better described by using polarization functions. The B3LYP method was run with the following triple-ζ basis sets like 6-311+G(d,p), 6-311++G(d,p), and 6-311G(3df,3pd) while the MP2 method the basis set used was 6-311++G(d,p). Whenever in the present paper no reference is explicitly provided concerning the model of computation to a specific computed molecular property, by default it should be considered to be B3LYP/6-311+G(d,p). The latter model is also consistent with our calculation that will be presented in a forthcoming paper dedicated to the substituted aminimides (larger molecules). Computed geometries, at B3LYP/6-311+G(d,p) and MP2(full)/6-311++G(d,p) levels, for the (*Z*) and (*E*) rotamers and for the RTS are virtually identical. However, the relative Gibbs free energy of the rotamers and the free energy of activation is ca. 1 kcal/mol larger when calculated with MP2 than with B3LYP. In this paper electronic structure will be discussed in terms of the Natural Bond Orbital (computed with NBO-3[41] and NBO-5[42,43]), which is closely associated with the familiar bonding concepts of Lewis. A brief summary of the terminology used in the present paper follows. In the NBO theory the input basis set is successively transformed into various localized basis sets. First, the input basis set is transformed to natural atomic orbitals (NAO).[44,45] Then, the NAO are transformed into natural hybrid orbitals (NHO).[46] Third, atom A could acquire a lone pair in the NHO (abbreviated throughout this paper as LP) or a localized σ or π bond (NBO) is formed between atom A and B as a result of the in-phase mixing of two NHO, namely h_A and h_B ($\sigma_{AB} = c_A h_A + c_B h_B$). The σ_{AB} is paired (to complete the span of the valence space) with a corresponding out-of-phase mixing of the same NHO ($\sigma^*_{AB} = c_B h_A - c_A h_B$). In the NBO jargon, orbitals such as LP, σ_{AB}, and π_{AB} are termed "Lewis" type or donor orbitals, and LP*, σ^*_{AB}, and π^*_{AB} are "non-Lewis" or acceptors. In an idealized Lewis structure the antibonds are empty. If LP*, σ^*_{AB}, or π^*_{AB} turn out to have occupancy (which is usually weak, no more than 0.5 e) this is an indication of "delocalization effects" which represent an irreducible departure from an idealized Lewis picture. In the NBO representation the diagonal elements of the Fock matrix represent the energies of localized bonds, lone pairs, and antibonds. Off-diagonal elements represent bond/antibond, lone pair/antibond, and antibond/antibond interactions. The net result of delocalization (e.g., electron transfer from donor to acceptor orbital) is an energetic stabilization that can be estimated by second-order perturbation theory (see Figure 1):

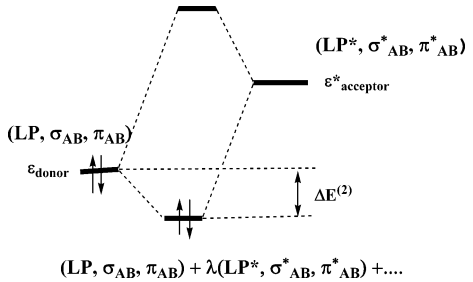

Figure 1. Donor−acceptor interaction diagram. $\Delta E^{(2)}$ is the second-order stabilization energy calculated from eq 1, which lowers the ϵ_{donor} energy level, and [(LP, σ_{AB}, and π_{AB}) + λ(LP*, σ^*_{AB}, and π^*_{AB})] is the corresponding "delocalized" molecular orbital incorporating the antibond "tail" through the weighing coefficient λ.

$$\Delta E^{(2)}_{i\rightarrow j^*} = -2\frac{\langle \sigma_i|\hat{H}|\sigma^*_j\rangle^2}{\epsilon_j^* - \epsilon_i} \qquad (1)$$

where $\hat{H}$ is the effective orbital Hamiltonian, ϵ_i is the donor NBO energy and ϵ^*_j is the acceptor NBO energy.

Finally, as a result of the "delocalization" the starting NBO acquires a weak antibond "tail". The "new" orbital termed Natural (semi-) Localized Molecular Orbital (NLMO)[47] is a linear combination of the parent Lewis-type NBO (LP, σ_i, π_i) and the (weak, λ as coefficient) contributions of the non-Lewis NBOs (LP*, σ^*_j, or π^*_j). Natural resonance theory (NRT)[48−50] provides the weight of the contributing Lewis structure to the DFT wave function.

Although partial atomic charge is frequently invoked in many papers, this concept is poorly defined.[51] Partial atomic charge is not a quantum observable. There are several procedures, definitively none of them accepted as the "best" for computing partial charges. Therefore, after comparing the outcome of several methodologies such as (i) Merz−Kollman−Singh (MKS)[52,53] electrostatic potential-derived charge, (ii) the Breneman−Wiberg (BW) model,[54] (iii) natural population analysis (NPA),[45] and (iv) Mulliken[55−58] population analysis, we have chosen in the present work to display only the MKS charges on the grounds that they mirror the charge on all atoms as illustrated by the chemical structure H-$CON^-N^+(CH_3)_3$. For example, NPA and Mulliken analyses predict a negative charge on the positive nitrogen atom. On the contrary, BW and MKS computed charges are positive on the ammonium nitrogen. Topological properties of the electron density were characterized by using the atoms-in-molecules (AIM)[29,59−63] methodology. The following relevant parameters at the bond critical points (BCP, e.g., saddle point in the density between two atoms) have been examined: charge density $\rho(\mathbf{r}_{BCP})$, Laplacian of the charge density $\nabla^2\rho(\mathbf{r}_{BCP})$, and bond ellipticity $\epsilon(\mathbf{r}_{BCP})$. Intramolecular hydrogen bonding CH- - -O═C was observed for one hydrogen of each of the two methyl groups cis to the carbonyl oxygen

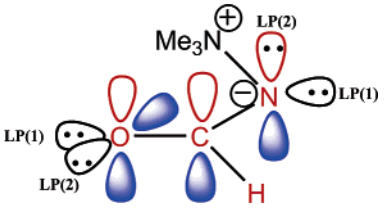

Figure 2. Oxygen and the negative nitrogen NBO lone pair assignments.

(see Figure 5). These weak hydrogen bonds have been characterized by the location of the bond and ring critical points, Laplacian of density, and ellipticity. All illustrations in Figure 4 are generated with GaussView 3.08, at isoval = 0.02, number of points 60, 49, 54, and resolution 0.333333, 0.333333, 0.333333. The lone pair assigment is displayed in Figure 2. LP(1) are the lower energy lone pairs on both oxygen ($sp^{0.62}$) and nitrogen ($sp^{1.12}$). LP(2) are the lone pairs of higher energy, both in p orbitals. On nitrogen, the p orbital is parallel to the π_{CO} orbital. The oxygen LP(2) orbital is perpendicular to the π_{CO} orbital. Note that for the oxygen lone pair orbitals, NBO analysis provides an alternative directionality[64−66] compared to the two equivalent sp^2 lone pair representation described in some textbooks.[67−70] The two descriptions are in fact equivalent.

Results and Discussion

We begin the discussion of our findings for the model compound $HCON^-N^+(CH_3)_3$ by displaying, for brevity, only the upper part of the electronic configuration and comparing it with that of related amides, anions of amides (amidates), and anions of hydrazides. Then, we examine the charge transfer from the LP(2) of N^- to the C═O group, which is in agreement as a trend with the Natural Resonance Theory analysis. Finally, we discuss the key metrics of the $O{=}C{-}N^-N^+$ functionality, the conformation, and the height of the rotational barrier around the $CO{-}N^-$ bond and provide a rationale for the conformational preference of formaminimide by examining the anatomy of those accountable interactions such as negative hyperconjugation, hydrogen bonding, and electrostatic attraction.

Electronic Structure of $HCON^-N^+(CH_3)_3$. The $-CON^-N^+$ functionality could be regarded as constructed from a C═O functionality that is "perturbed" by the N^-, just as the amide functionality, $-CONH_2$, is currently described as constructed from the interaction of C═O and $-NH_2$ groups. Undoubtedly, amides and aminimides are related, but one anticipates also dissimilarities. In both functionalities the C═O bond interacts with the electron donating nitrogen atom. However, in the amide the lone pair of the nitrogen that interacts with the carbonyl group is in a different charge environment. In amides the nitrogen is neutral, while in aminimides it is negative. Furthermore, we have included in Table 1, for the sake of comparison and to uncover specific facets regarding the mechanism by which the negative nitrogen interacts with the carbonyl, DFT computational results on amidate (amide anion) and the anion of hydrazide. Before presenting our results concerning the electronic and molecular structure of $H\text{-}CON^-N^+(CH_3)_3$ it is perhaps of interest to summarize the significant electronic features of the (seemingly) related amide bond. Traditionally, the electronic structure of amides is described by two major resonance contributors (**A** and **B**, see Scheme 1).[71,72] However, according to Wiberg and some other authors [54,73−87] the resonance structure **C** (not **B**) is a major contributor to the overall π electron charge distribution in amides, because the nitrogen preferentially transfers electron density to the vicinal carbon atom rather than to the whole $\pi_{C=O}$ bond, as is argued by the defenders of the classical view.[88−94]

SCHEME 1: Resonance Structure of Amides

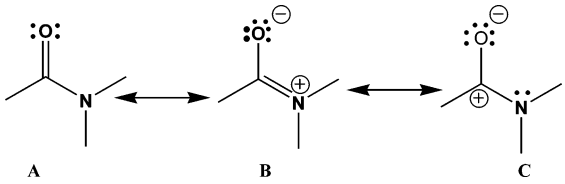

Because we regard amides as a reference for comparison with aminimide electronic structure, let us briefly review some of our computational (B3LYP/6-311+G(d,p)) results on the amide functionality. The calculated MKS electrostatic potential-derived charges for $H\text{-}CON(CH_3)_2$ in the ground and in the rotational transition state (RTS) state are given in Table 2. In the process of rotation around the CO−N bond the oxygen loses a minimal 0.031 e charge, while the carbonyl carbon releases 0.430 e. Rotation strongly influences the geometry of the amide function. In the RTS, when all π interaction is shut off, the C−N bond becomes 0.078 Å more elongated than in the ground state. Relatively less affected is the C═O bond, because the bond

TABLE 1: Energy (au) and Occupancy of Frontier NBOs (LUMO and HOMO), HOMO-1, HOMO-2, and HOMO-3 of Formaminimide and Some Congeners

			$HCON^-Me^b$		$HCON^-NMe_2{}^b$		$HCON^-N^+Me_3$	
NBO	H_2CO^a	$HCONMe_2{}^a$	*Z*	*E*	*Z*	*E*	*Z*	*E*
LUMO	π^*_{CO}	π^*_{CO}	π^*_{CN}	π^*_{CN}	π^*_{CN}	π^*_{CN}	π^*_{CO}	π^*_{CO}
energy	−0.018	0.010	0.225	0.220	0.219	0.209	0.031	0.041
occupancy	0.000	0.288	0.359	0.371	0.371	0.377	0.380	0.344
HOMO	$O_{LP(2)}$	$O_{LP(2)}$	$O_{LP(3)}$	$O_{LP(3)}$	$O_{LP(3)}$	$O_{LP(3)}$	$N^-_{LP(2)}$	$N^-_{LP(2)}$
energy	−0.296	−0.249	−0.026	−0.023	−0.037	−0.032	−0.187	−0.184
occupancy	1.878	1.984	1.633	1.621	1.633	1.613	1.577	1.605
HOMO-1	π_{CO}	$N_{LP(1)}$	$O_{LP(2)}$	$O_{LP(2)}$	$O_{LP(2)}$	$O_{LP(2)}$	$O_{LP(2)}$	$O_{LP(2)}$
energy	−0.414	−0.258	−0.032	−0.028	−0.046	−0.037	−0.226	−0.206
occupancy	1.999	1.666	1.881	1.873	1.875	1.875	1.871	1.850
HOMO-2		π_{CO}	π_{CN}	π_{CN}	π_{CN}	π_{CN}	π_{CO}	π_{CO}
energy		−0.368	−0.085	−0.089	−0.112	−0.101	−0.331	−0.324
occupancy		1.998	1.957	1.949	1.973	1.965	1.994	1.997
HOMO-3			$N^-_{LP(1)}$	$N^-_{LP(1)}$	$N_{LP(1)}$	$N_{LP(1)}$	$N^-_{LP(1)}$	$N^-_{LP(1)}$
NHO			($sp^{1.87}$)	($sp^{1.96}$)	($sp^{4.43}$)	($sp^{4.03}$)	($sp^{1.12}$)	($sp^{1.01}$)
energy			−0.139	−0.135	−0.117	−0.136	−0.410	−0.413
occupancy			1.918	1.894	1.872	1.894	1.941	1.936

[a] $O_{LP(2)}$ is a p NBO whose axis is coplanar with the $O{=}CH_2$ plane. $N_{LP(1)}$ ($HCONMe_2$) is a p NBO perpendicular to the OCN plane. [b] $O_{LP(3)}$ is a p NBO whose axis is perpendicular to the OCNN frame. $O_{LP(2)}$ is a p NBO whose axis is coplanar with the OCNN frame.

TABLE 2: MKS Electrostatic Potential Derived Charges on Oxygen, Carbon, and Negative Nitrogen, and C=O, C−N⁻, and N⁻−N⁺ Bond Distances in $HCON^-N^+(CH_3)_3$ and Some Congeners

compound	O	C	N⁻	C=O	CN⁻	N⁻−N⁺
$HCON(CH_3)_2$ ground state	−0.529	0.343	0.072	1.217	1.363	
TS ($\Delta G^{\ddagger} = 22.2$ kcal/mol)	−0.498	0.773	−0.457	1.201	1.441	
$HCON^-CH_3$						
(*Z*)	−0.857	0.912	−1.110	1.265	1.318	
(*E*)	−0.796	0.949	−1.103	1.247	1.325	
TS (above (*Z*) with $\Delta G^{\ddagger} = 24.4$ kcal/mol	−0.844	0.826	−0.915	1.254	1.316	
$HCON^-N(CH_3)_2$						
(*Z*)	−0.822	0.819	−0.822	1.260	1.325	1.444
(*E*)	−0.880	0.982	−0.732	1.252	1.329	1.454
TS (above (*Z*) with $\Delta G^{\ddagger} = 28.8$ kcal/mol)	−0.683	0.742	−0.760	1.236	1.355	1.438
$HCON^-N^+(CH_3)_3$						
(*Z*)	−0.706	0.669	−0.843	1.243	1.338	1.486
(*E*)	−0.625	0.716	−0.704	1.226	1.348	1.487
TS	−0.604	0.876	−0.817	1.219	1.392	1.429

contraction in the RTS is only −0.016 Å. In the ground state of amides the lone pair of the planar nitrogen is interacting (delocalized) with the π^* antibond of the C=O group. The partial charge transfer (0.288 e, see Table 1) from the lone pair of nitrogen will be directed mostly to the vicinal carbon atom, because it has the largest coefficient (0.8411) in the π^*_{CO} NBO, and much less to the oxygen, which has a smaller coefficient (0.5409). As a result of the charge transfer the second-order stabilization energy (see eq 1) is 64.4 kcal/mol. The highest occupied natural localized molecular orbital NLMO (HO-NLMO) is made up of 83.1% of the LP(1) of nitrogen NHO. The remainder is mostly the weak contribution (ca. 13%) of the π^*_{CO} NBO.

To assess the evolution of the π_{CO} in different nitrogen environments, NBO analyses have been carried out for $H\text{-}CON^-\text{-}CH_3$, $H\text{-}CON^-N(CH_3)_2$, and $H\text{-}CON^-N^+(CH_3)_3$. Compounds $H\text{-}CON^-CH_3$ and $H\text{-}CON^-N(CH_3)_2$ command attention due to their formal resemblance to the CON^- segment from $H\text{-}CON^-N^+\text{-}(CH_3)_3$. Remarkably, the computational results prove that π_{CO} (HOMO-2) no longer exists for $H\text{-}CON^-CH_3$ and $H\text{-}CON^-N\text{-}(CH_3)_2$. It is replaced by π_{CN} (see Table 1). The two anions are described by the **B** Lewis structure (Figure 3). For both anions the HOMO is occupied with the LP(3) and HOMO-1 with the LP(2) of the negative oxygen. The Gibbs free energy difference between the (*Z*) and (*E*) conformers is relatively larger for $H\text{-}CON^-CH_3$ ($\Delta G = 2.3$ kcal/mol) than for $H\text{-}CON^-N(CH_3)_2$ ($\Delta G = 0.34$ kcal/mol).

The next step is to attach to the CO the ylide segment $-N^-N^+$, to form $H\text{-}CON^-N^+(CH_3)_3$. By examining the NBOs, it is remarkable to note that π_{CO} has been restored. At this point let us clarify the electronic configuration of $H\text{-}CON^-N^+(CH_3)_3$. The computed "upper" part of the electronic configuration of $H\text{-}CON^-N^+(CH_3)_3$ is $...(N^-sp^{1.12})^2(\pi_{CO})^2(O_{LP(2)})^2(N^-_{LP(2)})^2$, where (see Figure 4) $N^-sp^{1.12}$ is the NHO on the negative nitrogen filled with the lower energy lone pair LP(1), π_{CO} is the carbonyl

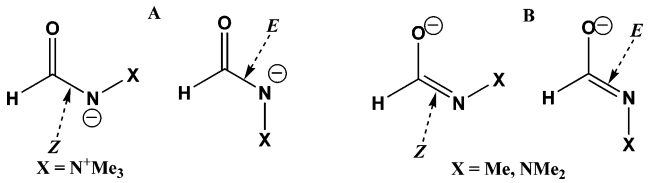

Figure 3. Conformational structure for (A) aminimides and (B) amidate and hydrazide anion.

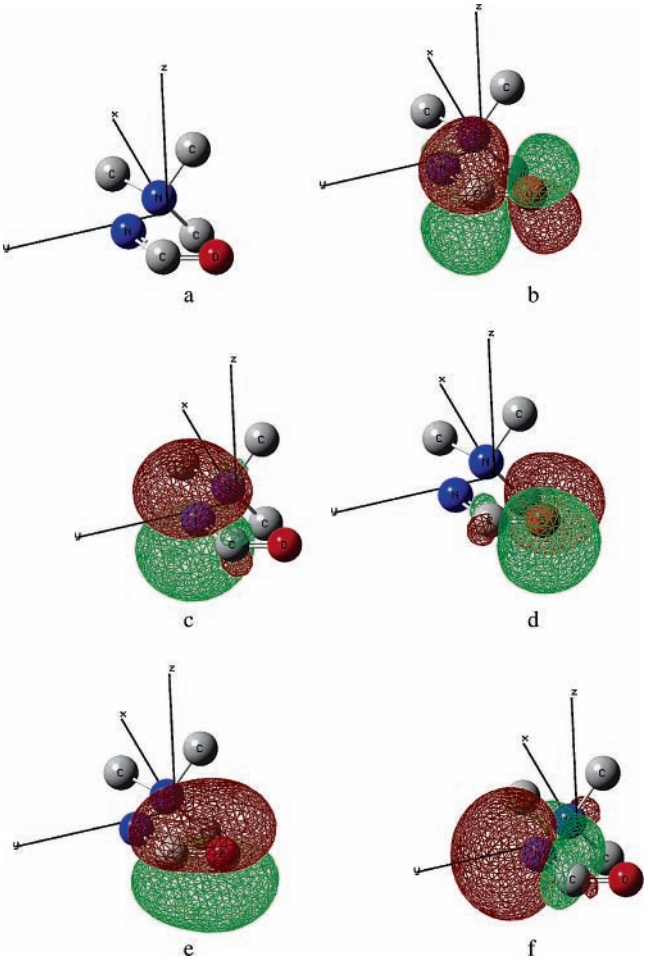

Figure 4. (a) The main atomic framework of (*Z*)-$HCON^-N^+(CH_3)_3$. For the sake of clarity hydrogen atoms were omitted. In b−f the main atomic frame is viewed from the same angle: (b) LUMO, π^*_{CO}; (c) HOMO (LP(2) of negative nitrogen); (d) HOMO-1, the oxygen LP(2) p NBO; (e) HOMO-2, $\pi_{CO} = 0.5078C_p + 0.8615O_p$ perpendicular to the OCN^-N^+ frameworkl; (f) HOMO-3, a $sp^{1.12}$ NBO located on the negative nitrogen atom.

π NHO, $O_{LP(2)}$ is the p NHO on the carbonyl oxygen that is perpendicular to the π_{CO}, and $N^-_{LP(2)}$ is the p NHO on the negative nitrogen occupied by the second nitrogen lone pair.

The first dissimilarity between $HCON^-N^+Me_3$ and $HCONMe_2$ is the fact that the HOMO's for the two compounds are different. In the case of the amide the HOMO NBO is the oxygen LP(2) orbital that lies orthogonal to the filled amide π_{CO} bond. The HOMO of $HCON^-N^+Me_3$ is the $LP(2)_{N^-}$ NBO occupied with an negative nitrogen lone pair (see Figure 4c). However, two NBOs are similar in $HCON^-N^+(CH_3)_3$ and $HCON(CH_3)_2$, namely LUMO NBO (π^*_{CO}) and HOMO-2 (π_{CO}).

A second dissimilarity between $HCON^-N^+(CH_3)_3$ and $HCON\text{-}(CH_3)_2$ is revealed by examining the data from Table 1 regarding the degree of nitrogen lone pair charge transfer. Thus $HCON^-N^+(CH_3)_3$ features a more "intense" charge transfer from nitrogen LP(2) to C=O than in $HCON(CH_3)_2$. The negative nitrogen donor transfers ca. 0.38 e into the π^*_{CO} acceptor, while in the amide $HCON(CH_3)_2$, the similar charge transfer from the nitrogen donor lone pair into the acceptor π^*_{CO} is only ca. 0.29 e. The more intense charge delocalization in aminimides than in amides is also supported by Natural Resonance Theory[49,50] (NRT) analysis by which the weights of various canonical structures are assessed. NRT predicts nearly equal weights of the resonance structures for the (*Z*)-formaminimide (see Scheme 2).

SCHEME 2: Leading NRT Structures for $HCON^{-}N^{+}(CH_3)_3$ Conformers and Their Corresponding Weights

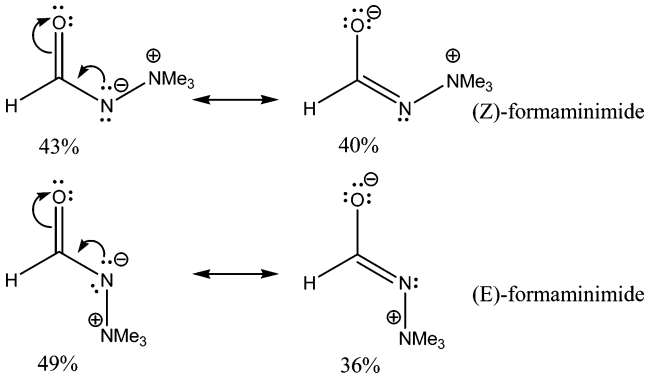

SCHEME 3: Leading NRT Structures for $HCON(CH_3)_2$ and Their Corresponding Weights

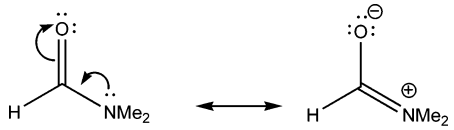

However, in the case of the (*E*)-formaminimide, the structure of the ylide with the negative nitrogen is significantly more important than that of the ylide with the negative oxygen (see Scheme 2). This result clearly suggests a configuration dependence of delocalization ability of the aminimide negative nitrogen.

For the sake of comparison, we have carried out similar NRT analysis for the dimethylformamide. Because neutral nitrogen transfers less charge to the CO function than the negative nitrogen, the classical representation outweighs the ionic structure by a margin of almost 2:1 (see Scheme 3).

A third dissimilarity is the fact that the gain in stabilization (see eq 1) as a result of the charge transfer is 100.3 kcal/mol for (*Z*)-$HCON^{-}N^{+}(CH_3)_3$, while in the case of $HCON(CH_3)_2$ the gain in stabilization is only 60 kcal/mol. Examination of Natural Localized Molecular Orbitals (NLMOs) resulting from the partial donation of the lone pair of nitrogen into the acceptor π^*_{CO} reveals that an antibond "tail" from a non-Lewis (delocalization) structure adds to the nitrogen lone pair NBO. Thus for $HCON^{-}N^{+}(CH_3)_3$ in the highest occupied NLMO the original NBO nitrogen LP(2) contribution is 78.8% (*Z conformer*) and 80.2% (*E conformer*), respectively, compared to the *N*,*N*-dimethylformamide NLMO in which 83% of the nitrogen LP(2) NBO is preserved.

A short comment on the role of the positive nitrogen is pertinent here. In contrast to amidate and hydrazide anions, the π_{CO} NBO is restored in (*Z*)-$HCON^{-}N^{+}(CH_3)_3$. This fact is attributable to the electron-withdrawing ammonium cation ($-N^{+}(CH_3)_3$) substituent linked to the negative nitrogen. It was observed by X-ray photoelectron spectroscopy that the electron density on this ammonium nitrogen is larger than that in ammonium salts.[95−97] This means that the σ electrons in the $N^{-}-N^{+}$ bond are more displaced toward the positive nitrogen and thus diminish the ability of the negative nitrogen to transfer charge into the π^*_{CO}. In the amidate and the hydrazide anion the lack of the ammonium withdrawing substituent on the negative nitrogen makes possible more charge transfer, which ultimately gives rise to the formation of a π_{CN} bond.

The Key Metrics and the Conformation of H-$CON^{-}N^{+}(CH_3)_3$. There are two remarkable features in the computed geometry of (*Z*)-H-$CON^{-}N^{+}(CH_3)_3$: (i) the relatively long C═O bond distance and (ii) the strong preference for the (*Z*) configuration around the C−N^{-} bond. Unfortunately, there are only three experimental CO bond distances for aminimides available in the literature.[98−101] All of them are for aryl-substituted aminimides (Ar-$CON^{-}N^{+}(CH_3)_3$ and C_6H_5-$CON^{-}N^{+}(CH_2CHOHCH_3)(CH_3)_2$). The X-ray determined CO bond distance interval is 1.243−1.258 Å, longer than a normal C═O bond and reminiscent of the C═O bond length of urea (1.265 Å).[102,103] The computed (at B3LYP and MP2 levels) carbonyl bond lengths in (*Z*)-H-$CON^{-}N^{+}(CH_3)_3$ are in the interval of 1.238−1.246 Å (see Table 3), which is very close to the X-ray determined value by Cameron[98,99] for (*Z*)-C_6H_5-$CON^{-}N^{+}(CH_3)_3$ and to our results[101] for (*Z*)-C_6H_5-$CON^{-}N^{+}(CH_2CHOHCH_3)(CH_3)_2$, but shorter[100] than the value for (*Z*)-ClC_6H_4-$CON^{-}N^{+}(CH_3)_3$. Interestingly, the computed carbonyl bond length in (*E*)-H-$CON^{-}N^{+}(CH_3)_3$ is shorter than that in (*Z*)-H-$CON^{-}N^{+}(CH_3)_3$ and is similar to the carbonyl distance in H-$CON(CH_3)_2$. This results from the fact that more electron density is transferred into the carbonyl group of the (*Z*)-H-$CON^{-}N^{+}(CH_3)_3$ conformer (weakening the CO bond) than in the case of the (*E*) rotamer. The computed value for the bond CO−N^{-} in (*Z*)-$HCON^{-}N^{+}(CH_3)_3$ is 1.330 Å, shorter than the CO−N bond distance of both H-$CON(CH_3)_2$ (experimental 1.391 Å,[104] computed here to be 1.363 Å) and the hydrazide $C_6H_5CON(CH_3)N(CH_3)_2$ (experimental 1.343 Å,[105] computed here to be 1.383 Å). The shortening of this particular bond in aminimides is clearly due to a larger degree of electron transfer from the LP(2) of the negative nitrogen into the π^*_{CO}.

The (*Z*)- and (*E*)-H-$CON^{-}N^{+}(CH_3)_3$ rotamers around the CO−N^{-} bond (see Figure 3A) have different thermodynamic stability. (*Z*)-$HCON^{-}N^{+}(CH_3)_3$ is thermodynamically more stable than (*E*)-$HCON^{-}N^{+}(CH_3)_3$. The calculated Gibbs energy gap, ΔG, is 11.7 kcal/mol at the B3LYP/6-311+G(d,p) level of theory and 12.9 kcal/mol at the MP2(full)/6-311++G(d,p) level. The fact that acyclic aminimides assume only the (*Z*) conformation is in agreement with X-ray measurements[98−101] and dipole moment studies.[106] What makes the (*Z*) configuration relatively more stable?

(i) The prominent factor that makes (*Z*)-$HCON^{-}N^{+}(CH_3)_3$ thermodynamically more stable is the more favorable interaction environment in the (*Z*) than in the (*E)* conformer for the N^{-} $sp^{1.12}$ lone pair to interact with various σ^* acceptors (negative hyperconjugation) and Rydberg* antibonds. The magnitudes are assessed by deleting all the off-diagonal elements in the Fock matrix resulting from the $LP(1)_{N^-}$ interactions with the acceptors antibonds. Thus, there is a loss of stability (meaning a stronger effect) for the (*Z*) conformer of 60.7 kcal/mol versus of 51.6 kcal/mol for the (*E*) conformer. Therefore, out of the total 12 kcal/mol difference in stability (see Figure 6), ca. 9 kcal/mol is accounted for due to the negative hyperconjugation. In what concerns specific interactions, for example, in the (*Z*) conformer, the most notable is the anti-periplanar interaction of the nitrogen lone pair LP(1) with the acceptor σ^*_{CO} NBO.

(ii) The next factor, C═O···H−CH_2N^{+} hydrogen bonding, accounts for less than 25% of the energy gap between the (*Z*) and (*E)* conformer, respectively.

Such bonds are nicely and firmly revealed by AIM analysis. Indeed, two hydrogen bonding interactions occur between hydrogens, one from each CH_3 group that is properly oriented with the oxygen atom (see Figure 5). For both $N^{+}C-H\cdots O=C$ hydrogen bonds at the bond critical point the charge density $\rho(\mathbf{r}_{BCP})$ is 0.01767 au, the Laplacian of the charge density $\nabla^2\rho(\mathbf{r}_{BCP})$ is 0.06146 au, and the bond ellipticity $\epsilon(\mathbf{r}_{BCP})$ is

TABLE 3: Calculated Bond Distances (Å) and Bond Angles (degree) in (*Z*)-, (*E*)-, and RTS-HCON$^-$N$^+$(CH$_3$)$_3$

compound	C═O	C(O)−N	N−N	O−C−N	C−N−N
1. (*Z*)-HCON$^-$N$^+$(CH$_3$)$_3$					
B3LYP/6-311+G(d,p)	1.243	1.330	1.480	130.84	113.22
B3LYP/6-311++G(d,p)	1.243	1.338	1.487	130.84	113.08
B3LYP/6-311++G(3df,3pd)	1.238	1.335	1.481	130.91	112.87
MP2(full)/6-311++G(d,p)	1.246	1.345	1.465	130.43	112.46
5. (*E*)-HCON$^-$N$^+$(CH$_3$)$_3$					
B3LYP/6-311+G(d,p)	1.226	1.340	1.480	124.12	113.20
B3LYP/6-311++G(d,p)	1.226	1.348	1.487	124.12	113.06
B3LYP/6-311++G(3df,3pd)	1.219	1.347	1.480	124.13	113.30
MP2(full)/6-311++G(d,p)	1.231	1.354	1.463	124.23	112.44
6. RTS-HCON$^-$N$^+$(CH$_3$)$_3$					
B3LYP/6-311+G(d,p)	1.219	1.392	1.429	126.11	114.34
B3LYP/6-311++G(d,p)	1.219	1.392	1.429	126.10	114.34
B3LYP/6-311++G(3df,3pd)	1.213	1.389	1.422	126.05	114.54
MP2(full)/6-311++G(d,p)	1.226	1.398	1.428	125.86	111.62

0.1868. The low value of the $\rho(\mathbf{r}_{BCP})$ and the positive sign and the $\nabla^2\rho(\mathbf{r}_{BCP})$ are typical for weak interactions such as hydrogen bonding.[107,108] Two six-membered rings comprising the hydrogen bonding are formed from O═C−N$^-$−N$^+$−C−H atoms (one C−H from each methyl group). Obviously, the hydrogen bonds that are stabilizing the (*Z*) conformation are missing in the (*E*) structure. How does the weak hydrogen bonding arise? Intuitively, the more acidic the proton donor (in our case from methyl C−H) and the more basic the acceptor (aminimide carbonyl oxygen) the stronger is the hydrogen bond. As a result of LP(2)$_{N^-}$ donation the proton acceptor group (the oxygen from the CO) has relatively higher electron density (see Table 2). Because the CH is linked to the quaternary N$^+$ atom (a strong electron withdrawing atom), the net result is that protons from the methyl groups are relatively depleted of electron density, thus making the C−H a better proton donor. Our finding

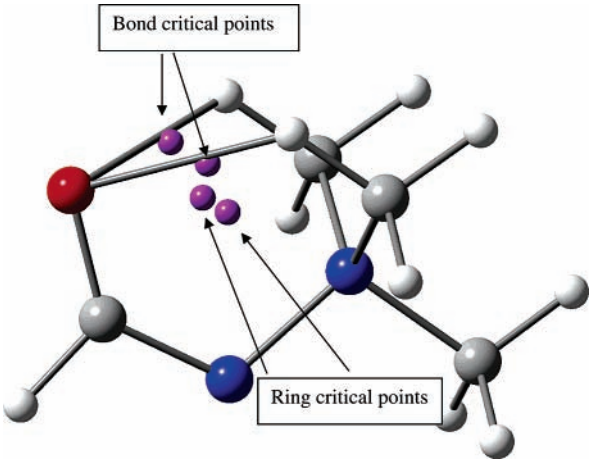

Figure 5. C−H- - -O═C interactions and location of bond and ring critical points in (*E*)-HCON$^-$N$^+$(CH$_3$)$_3$. The H (white balls)- - -O (red ball) bonds are depicted together with the location of the bond and ring critical points (magenta).

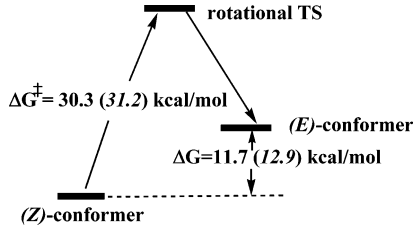

Figure 6. Calculated Gibbs free energies at 25 °C (B3LYP/6-311+G(d,p) and MP2(full)/6-311++G(d,p), in parentheses, in italics) for (*E*)-HCON$^-$N$^+$(CH$_3$)$_3$ and the RTS connecting the two conformations relative to (*Z*)-HCON$^-$N$^+$(CH$_3$)$_3$.

parallels Houk's[109,110] conclusion concerning the importance of R$_3$N$^+$C−H···O═C hydrogen bonding in conformational analysis. The computed bond distances (2.236 Å) in the case of (*Z*)-HCON$^-$N$^+$(CH$_3$)$_3$ are shorter than the sum of the van der Waals radii of C−H (ca. 1.2 Å) and C═O (1.5 Å).[111] Historically, such a weak C−H···O hydrogen bond had been suggested by Glasstone[112] more than 60 years ago. Yet, for many years this idea has been abandoned[113] and even disputed. Conclusive evidence regarding the existence of the C−H···O hydrogen bond in crystals came in 1982, when Taylor and Kennard[111] published their survey of crystallographic data. Presently, C═O···H bonding is increasingly recognized as a structural element in chemistry[114−122] and biology.[123] The weak C−H···O═C bond is estimated to be half the strength of the N−H···O═C bond.[124] This means that the two C−H···O═C hydrogen bonds in (*Z*)-HCON$^-$N$^+$(CH$_3$)$_3$ are equivalent in strength to a N−H···O═C bond.

(iii) There is more electron transfer from the LP(2) of the negative nitrogen into the π^*_{CO} for the (*Z*) conformer (0.385 e) than for the (*E*) conformer (0.344 e). As a result of relatively more charge transfer, the "tail" π^*_{CO} ($\pi^*_{CO} = 0.8615C_p - 0.5078O_p$) in the (*Z*) conformer HO-NLMO is relatively larger than that for the (*E*) conformer. Consequently, the CO−N$^-$ bond in the (*Z*) conformer (1.338 Å) becomes shorter (stronger) than that for the (*E*) conformer (1.348 Å). The donor−acceptor stabilization (eq 1) is 100.3 kcal/mol for the (*Z*) conformer and only 85.0 kcal/mol for the (*E*) conformer.

(iv) The (*Z*) configuration enhances the favorable electrostatic interactions by bringing the oppositely charged atoms closer together and the negatively charged atoms further apart. In the (*Z*) configuration the negative nitrogen LP(1) occupying the sp$^{1.12}$ hybrid NBO is relatively more distant (trans configuration) from the partially negatively charged oxygen than it is in the (*E*) configuration. Further, the attractive interaction between the partially negatively charged oxygen and the N$^+$ atom is larger in the (*Z*) configuration than in the (*E*) configuration.

The Rotational Barrier in HCON$^-$N$^+$Me$_3$. Isomerization of the (*Z*)-HCON$^-$N$^+$(CH$_3$)$_3$ to the (*E*)-HCON$^-$N$^+$(CH$_3$)$_3$ conformer occurs through a rotational transition structure (RTS) in which the C═O makes a dihedral angle approximately of 90° with the N$^-$N$^+$ bond. Consequently, in the RTS the LP(2)$_{N^-}$/π^*_{CO} interaction is turned off. The computed rotational barrier ($\Delta G^‡$ at 25 °C) in going from (*Z*)-HCON$^-$N$^+$(CH$_3$)$_3$ to (*E*)-HCON$^-$N$^+$(CH$_3$)$_3$ is 30.3 (B3LYP/6-311+G(d,p)) and 31.2 kcal/mol (MP2(full)/6-311++G(d,p)). Compared to HCON(CH$_3$)$_2$ it is larger by about 8−12 kcal/mol.[125−127] The greater rotational barrier in aminimides occurs because rotation of the

SCHEME 4: Leading NRT Structures for HCON−R (Amidates, X = CH_3; Hydrazide Anions, X = $N(CH_3)_2$) and Their Corresponding Weights

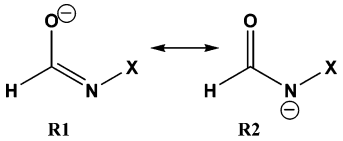

X	R1	R2
CH_3	50%	38%
$N(CH_3)_2$	46%	35%

C═O bond relative to the N^-−N^+ bond causes the relatively stronger CN bond to be broken.

The height of the computed activation barrier for the conversion of the (*Z*) to the (*E*) conformer and the difference in energy among the conformers provides a reasonable explanation to understanding the failure of variable-temperature NMR to interconvert the two conformers. In the −80 to +110 °C range, the ^{1}H NMR of (*Z*)-$C_6H_5CON^-N^+(CH_3)_3$ is virtually unchanged.[99] Unfortunately, the temperature cannot be raised further because aminimides undergo N^-N^+ bond cleavage, rearrangements and elimination reactions near their melting point.[128−130]

In the RTS the HOMO NBO is overwhelmingly a p orbital, contaminated with 13% s orbital (actually a $sp^{6.74}$ NHO), which is rotated to ∼90° with respect to the π_{CO} NBO plane. The LP-(1) of the negative nitrogen fills a $sp^{1.74}$ hybrid NBO (HOMO-2) parallel to the π_{CO}. Although geometrically the HOMO-2 is correctly oriented in the RTS to interact (donate) with the π^*_{CO} orbital, the LP(1) of N^- is only slightly delocalized into the C═O antibond. The relatively lower energy level of the LP(1) is responsible for the diminished interaction with the π^*_{CO} orbital. Thus, the donation of the negative nitrogen LP(1) $sp^{1.74}$ hybrid into the acceptor (π^*_{CO}) brings about only 14.3 kcal/mol in stabilization.

What are the effects of turning off the $LP(2)_N$-/π^*_{CO} interaction? First, in RTS-$HCON^-N^+(CH_3)_3$ there is a shortening of the C═O bond and a lengthening of the C−N bond (see Table 2). The C−N bond length increase is more substantial than the shortening of the C═O bond. This trend is reminiscent of amides;[131,132] however, in the latter this effect is relatively larger. Moreover, as a result of the rotation around the O═C−N bond, the relative charge changes of the carbonyl carbon and the carbonyl oxygen display similar trends in aminimides and amides. Thus, the MKS electrostatic potential derived charge on the carbonyl carbon in RTS-$HCON^-N^+(CH_3)_3$ becomes more positive than that for (*Z*)-$HCON^-N^+(CH_3)_3$, while the "positivation" of the oxygen is approximately half of that of the carbon. As is illustrated in Table 2, in RTS of $HCON(CH_3)_2$ the carbon becomes substantially more positive than the oxygen compared to the electrostatic charges of the respective carbonyl atoms in the ground state.

Structures with negative nitrogen linked to a CO group such as $HCON^-R$ (amidates, R = CH_3; hydrazide anions R = $N(CH_3)_2$) should be formally more closely related to $HCON^-N^+(CH_3)_3$ than to amides. For example, similarly to the case of $HCON^-N^+(CH_3)_3$, the two nitrogen lone pairs in $HCON^-CH_3$ and $HCON^-N(CH_3)_2$ fill a p NBO and a hybrid sp NBO, respectively, with the two orbitals oriented orthogonal to each other. However, in $HCON^-CH_3$ and $HCON^-N(CH_3)_2$ (unlike formaminimide) the leading resonance structure, **R1**, has a C═N bond (see Scheme 4).

In formaminimide the strong electron withdrawing group $N^+(CH_3)_3$ is modulating the ability of the negative nitrogen to donate electrons to the C═O bond such as to make the **R2** structure (X = $N^+(CH_3)_3$) the leading resonance structure.

Conclusions. We explored the geometric and the electronic structure of formaminimides using two levels of theory: B3LYP (basis set 6-311+G(d,p), 6-311++G(d,p), 6-311G(3df,3pd)) and MP2(full)/6-311++G(d,p). There are no significant differences in the predicted geometries of formaminimides as a function of computational level DFT or ab initio Hartree−Fock, or basis set size. However, for the free energy difference between the (*Z*)-$HCON^-N^+(CH_3)_3$ and (*E*)-$HCON^-N^+(CH_3)_3$ rotamers and the height of the energy barrier for conversion of (*Z*) into (*E*) rotamer, MP2 predicts ca. 1 kcal/mol larger difference than B3LYP in both relative stability and free energy of activation. The major stabilizing factor of the (*Z*) configuration, negative hyperconjugation (such as delocalization of the N^- $sp^{1.12}$ lone pair into σ^*_{CO}), accounts for ca. 75% of the ca. 12 kcal/mol that separates the two rotamers. The remainder of the stabilization energy is provided by two other factors: (1) the two intramolecular hydrogen bonds between the carbonyl oxygen and the C−H bonds, each one from a different ammonium methyl group, and (2) the favorable electrostatic interaction between the ammonium nitrogen and the enriched carbonyl oxygen by electron donation from the negatively charged nitrogen. The calculated upper electronic configuration of (*Z*)-formaminimides is as follows. The HOMO is the p orbital of the negative nitrogen parallel to the π_{CO}, while the second lone pair of nitrogen is in an sp hybrid (HOMO-3) lying in the plane of the OCNN framework. HOMO-1 comprises the oxygen lone pair and HOMO-2 is the π_{CO}. Charge transfer from $HCON^-N^+(CH_3)_3$ assumes a (*Z*) configuration around the CO−N^-N^+ bond. The (*E*) conformer is less stable thermodynamically. Because of the stronger C−N^- bond, we predict that interconversion of the (*Z*) conformer into the (*E*) conformer requires 1.5 times more energy than for an identically substituted amide. The Natural Resonance Theory analysis predicts that for formaminimide the canonical ylide structure with negative nitrogen has nearly equal weight with the ylide structure with negative oxygen, indicating the enhanced ability of the negative nitrogen of aminimides to donate electrons relative to the neutral nitrogen of amides.

Acknowledgment. M.D.G. is grateful to the MIT Chemistry Department for support.

Supporting Information Available: A listing of optimized geometries and energies for (*Z*), (*E*), and rotational TS of $HCON^-N^+Me_3$ and a summary of relevant NBO-5 results (NBO, second-order perturbation, Natural Resonance Theory). This material is available free of charge via the Internet at http://pubs.acs.org.

References and Notes

(1) Hellwinkel, D. *Systematic Nomenclature of Organic Chemistry*; Springer-Verlag: Berlin, Germany, 2001; pp 96 and 3.9.

(2) We are grateful to Prof. Dr. D. Hellwinkel (Organish-Chemisches Institut, Universitat Heidelberg) for suggesting the scientific name that appears in the title of the present paper. These compounds are currently known in the literature as aminimides (more often) or, less frequently, as *N*-ammonioamidates.

(3) Hinman, R. L.; Flores, M. C. *J. Org. Chem.* **1959**, *24*, 660−664.

(4) Illien, B.; Berthelot, M.; Morris, D. G.; Laurence, C. *J. Phys. Org. Chem.* **2000**, *13*, 293−299.

(5) Rutenber, E. E.; McPhee, F.; Kaplan, A. P.; Gallion, S. L.; Hogan, J. C., Jr.; Craik, C. S.; Stroud, R. M. *Bioorg. Med. Chem.* **1996**, *4*, 1545−1558.

(6) Wawzonek, S.; Yeakey, E. *J. Am. Chem. Soc.* **1960**, *82*, 5718−5721.

(7) Koenig, K. H.; Kummer, H.; Jung, J. Badische Anilin & Soda Fabrik AG, German Patent DE 1809950, Nov. 20, 1968.

(8) Kabara, J. J.; Haitsma, G. V. *J. Am. Oil Chem. Soc.* **1975**, *52*, 444−447.
(9) Kabara, J. J. *J. Am. Oil Chem. Soc.* **1977**, *54*, 202−206.
(10) Kabara, J. J.; Vrable, R.; Ikeda, I.; Okahara, M. *J. Am. Oil Chem. Soc.* **1977**, *54*, 316−318.
(11) Kabara, J. J.; McKillip, W. J.; Sedor, E. A. *J. Am. Oil Chem. Soc.* **1975**, *52*, 316−317.
(12) Tichniouin, M.; Sauleau, J.; Sauleau, A.; Lacroix, P. *Eur. J. Med. Chem.* **1982**, *17*, 265−270.
(13) Colombo, M.; Farre, A. J.; Fort, M.; Martinez, L.; Roser, R.; Sagarra, R. *Methods Find. Exp. Clin. Pharmacol.* **1987**, *9*, 101−110.
(14) Tsuchiya, S.; Seno, M. *J. Phys. Chem.* **1994**, *98*, 13680−13686.
(15) Hartlage, J. A.; McKillip, W. J. Archer-Daniels-Midland Co., FR French Patent 1505771, 1967.
(16) Inubushi, S.; Ikeda, T.; Tazuke, S.; Satoh, T.; Kumagai, Y. *J. Polym. Sci., Part A*: *Polym. Chem.* **1988**, *26*, 1779−1789.
(17) McKillip, W. J. *Adv. Urethane Sci. Technol.* **1974**, *3*, 81−107.
(18) McKillip, W. J.; Culbertson, B. M.; Gynn, G. M.; Menardi, P. J. *Ind. Eng. Chem. Prod. Res. Dev.* **1974**, *13*, 197−201.
(19) Mehta, A. C.; Rickter, D. O.; Kolesinski, H. S.; Taylor, L. D. *J. Polym. Sci., Part A*: *Polym. Chem.* **1983**, *21*, 1159−1164.
(20) Niino, H.; Noguchi, S.; Nakano, Y.; Tazuke, S. *J. Appl. Polym. Sci.* **1982**, *27*, 2361−2368.
(21) Slagel, R. C.; Bloomquist, A. E. *Can. J. Chem.* **1967**, *45*, 2625−2628.
(22) Throckmorton, P. E.; Luckman, E. R. *Rubber Chem. Technol.* **1980**, *53*, 270−284.
(23) Carleton, P. S.; Lockwood, R. J.; Reymore, H. E., Jr. Upjohn Co., USA, U.S. Patent 3,925,284, December 9, 1975.
(24) Matsueda, K.; Noguchi, S.; Niino, H.; Nakano, Y. Mitsubishi Petrochemical Co., Ltd., Japan; Permachem. Asia, Ltd., Application: JP Patent 73-115690, Nov. 17, 1973, p 14 ff.
(25) In *The Amide Linkage*: *Selected Structural Aspects in Chemistry, Biochemistry, and Material Science*; Greenberg, A., Breneman, C. M., Liebman, J. F., Eds.; Wiley: New York, 2000.
(26) Lutsyk, A.; Suikov, S.; Bondarenko, A.; Pechtereva, T. *Monatsh. Chem.* **2003**, *134*, 1333−1339.
(27) Kirino, M.; Sanda, F.; Endo, T. *J. Polym. Sci., Part A*: *Polym. Chem.* **2000**, *38*, 3428−3433.
(28) Smith, G. T.; Mallinson, P. R.; Frampton, C. S.; Howard, J. A. K. *J. Chem. Soc., Perkin Trans.* **1997**, 1329−1331.
(29) Bader, R. F. W. *Atoms in Molecules*: *A Quantum Theory*; Oxford University Press: Oxford, UK, 1990.
(30) Frisch, M. J.; Trucks, G. W.; Schlegel, H. B.; Scuseria, G. E.; Robb, M. A.; Cheeseman, J. R.; Zakrzewski, V. G.; Montgomery J. A., Jr.; Stratmann, R. E.; J. C. Burant; Dapprich, S.; Millam, J. M.; Daniels, A. D.; Kudin, K. N.; Strain, M. C.; Farkas, O.; Tomasi, J.; Barone, V.; Cossi, M.; Cammi, R.; Mennucci, B.; Pomelli, C.; Adamo, C.; Clifford, S.; Ochterski, J.; Petersson, G. A.; Ayala, P. Y.; Cui, Q.; Morokuma, K.; Malick, D. K.; Rabuck, A. D.; Raghavachari, K.; Foresman, J. B.; Cioslowski, J.; Ortiz, J. V.; Baboul, A. G.; Stefanov, B. B.; Liu, G.; Liashenko, A.; Piskorz, P.; Komaromi, I.; Gomperts, R.; Martin, R. L.; Fox, D. J.; Keith, T.; Al-Laham, M. A.; Peng, C. Y.; Nanayakkara, A.; Challacombe, M.; Gill, P. M. W.; Johnson, B.; Chen, W.; Wong, M. W.; Andres, J. L.; Gonzalez, G.; Head-Gordon, M.; Replogle, E. S.; Pople, J. A. *Gaussian 98*, Revision A.9; Gaussian: Pittsburgh, PA, 1998.
(31) Frisch, M. J.; Trucks, G. W.; Schlegel, H. B.; Scuseria, G. E.; Robb, M. A.; Cheeseman, J. R.; Montgomery J. A., Jr.; Vreven, T.; Kudin, K. N.; Burant, J. C.; Millam, J. M.; Iyengar, S. S.; Tomasi, J.; Barone, V.; Mennucci, B.; Cossi, M.; Scalmani, G.; Rega, N.; Petersson, G. A.; Nakatsuji, H.; Hada, M.; Ehara, M.; Toyota, K.; Fukuda, R.; Hasegawa, J.; Ishida, M.; Nakajima, T.; Honda, Y.; Kitao, O.; Nakai, H.; Klene, M.; Li, X.; Knox, J. E.; Hratchian, H. P.; Cross, J. B.; Adamo, C.; Jaramillo, J.; Gomperts, R.; Stratmann, R. E.; Yazyev, O.; Austin, A. J.; Cammi, R.; Pomelli, C.; Ochterski, J.; Ayala, P. Y.; Morokuma, K.; Voth, G. A.; Salvador, P.; Dannenberg, J. J.; Zakrzewski, V. G.; Dapprich, S.; Daniels, A. D.; Strain, M. C.; Farkas, O.; Malick, D. K.; Rabuck, A. D.; Raghavachari, K.; Foresman, J. B.; Ortiz, J. V.; Cui, Q.; Baboul, A. G.; Clifford, S.; Cioslowski, J.; Stefanov, B. B.; Liu, G.; Liashenko, A.; Piskorz, P.; Komaromi, I.; Martin, R. L.; Fox, D. J.; Keith, T.; Al-Laham, M. A.; Peng, C. Y.; Nanayakkara, A.; Challacombe, M.; Gill, P. M. W.; Johnson, B.; Chen, W.; Wong, M. W.; Gonzalez, G.; Pople, J. A. In *Gaussian 03*, Revision B.04; Gaussian: Pittsburgh, PA, 2003.
(32) Parr, R. G.; Yang, W. *Density-Functional Theory of Atoms and Molecules*; Oxford University Press: New York, 1989.
(33) Parr, R. G., Ed. *Density-Functional Theory of Atoms and Molecules*; Oxford University Press: New York, 1995.
(34) Moller, C.; Plesset, M. S. *Phys. Rev.* **1934**, *46*, 618−622.
(35) Koch, W.; Holthausen, M. C. *A Chemist's Guide to Density Functional Theory*; Wiley-VCH: Weinheim, Germany, 2001; p 82.
(36) Cramer, C. J. *Essentials of Computational Chemistry*: *Theories and Models*; Wiley: Chichester, England, 2002; p 251.
(37) Becke, A. D. *J. Chem. Phys.* **1993**, *98*, 5648−5652.
(38) Lee, C.; Yang, W.; Parr, R. G. *Phys. Rev. B*: *Condens. Matter Mater. Phys.* **1988**, *37*, 785−789.
(39) Chandrasekhar, J.; Andrade, J. G.; Schleyer, P. v. R. *J. Am. Chem. Soc.* **1981**, *103*, 5609−5612.
(40) Foresman, J. B.; Frisch, E. *Exploring Chemistry with Electronic Structure Methods*, 2nd ed.; Gaussian: Pittsburgh, PA, 1996; p 99.
(41) Glending, E. D.; Reed, A. E.; Carpenter, J. E.; Weinhold, F. *Gaussian NBO*, Version 3.1; see also: (a) Foster, J. P.; Weinhold, F. *J. Am. Chem. Soc.* **1980**, *102*, 7211−7218. (b) Reed, A. E.; Curtiss, L. A.; Weinhold, F. *Chem. Rev.* **1988**, *88*, 899−926. (c) Weinhold, F.; Landis, C. R. *Chem. Ed. Res. Pract.* **2001**, *2*, 91−104. (d) Weinhold, F. Natural Bond Orbital Methods. In *Encyclopedia of Computational Chemistry*; Schleyer, P. v. R., Allinger, N. L., Clark, T., Gasteiger, J., Kollman, P. A., Schaefer, H. F., III, Schreiner, P. R., Eds.; Wiley: Chichester; UK, 1998; pp 1792−1811. (e) http://www.chem.wisc.edu/∼nbo5/WhyNBO.htm. (f) Weinhold, F.; Carpenter, J. E. In *The Structure of Small Molecules and Ions*; Naaman, R., Vager, Z., Eds.; Plenum: New York; 1988; pp 227−236.
(42) Glendening, E. D.; J. K. B.; Reed, A. E.; J. E. Carpenter, J. E.; J. A. B.; Morales, C. M.; Weinhold, F. *NBO 5.0*; Theoretical Chemistry Institute, University of Wisconsin: Madison, WI, 2001); http://www.chem.wisc.edu/∼nbo5.
(43) Weinhold, F. *Abstracts of Papers*; 222nd National Meeting of the American Chemical Society, Chicago, IL, August 26−30, 2001; American Chemical SOciety: Washington, DC, 2001; PHYS-110.
(44) Reed, A. E.; Weinhold, F. *J. Chem. Phys.* **1983**, *78*, 4066−4073.
(45) Reed, A. E.; Weinstock, R. B.; Weinhold, F. *J. Chem. Phys.* **1985**, *83*, 735−746.
(46) Foster, J. P.; Weinhold, F. *J. Am. Chem. Soc.* **1980**, *102*, 7211−7218.
(47) Reed, A. E.; Weinhold, F. *J. Chem. Phys.* **1985**, *83*, 1736−1740.
(48) Glendening, E. D.; Badenhoop, J. K.; Weinhold, F. *J. Comput. Chem.* **1998**, *19*, 628−646.
(49) Glendening, E. D.; Weinhold, F. *J. Comput. Chem.* **1998**, *19*, 610−627.
(50) Glendening, E. D.; Weinhold, F. *J. Comput. Chem.* **1998**, *19*, 593−609.
(51) Cramer, C. J. *Essentials of Computational Chmistry*: *Theories and Models*; John Wiley & Sons Ltd: Baffin Lane, Chichester, England, 2002; p 278.
(52) Besler, B. H.; Merz, K. M., Jr.; Kollman, P. A. *J. Comput. Chem.* **1990**, *11*, 431−439.
(53) Singh, U. C.; Kollman, P. A. *J. Comput. Chem.* **1984**, *5*, 129−145.
(54) Breneman, C. M.; Wiberg, K. B. *J. Comput. Chem.* **1990**, *11*, 361−373.
(55) Mulliken, R. S. *J. Chem. Phys.* **1955**, *23*, 1833−1840.
(56) Mulliken, R. S. *J. Chem. Phys.* **1955**, *23*, 1841−1846.
(57) Mulliken, R. S. *J. Chem. Phys.* **1955**, *23*, 2338−2342.
(58) Mulliken, R. S. *J. Chem. Phys.* **1955**, *23*, 2343−2346.
(59) Cioslowski, J.; Surjan, P. R. *Theochem* **1992**, *87*, 9−33.
(60) Bader, R. F. W. *Chem. Rev.* **1991**, *91*, 893−928.
(61) Cioslowski, J.; Nanayakkara, A.; Challacombe, M. *Chem. Phys. Lett.* **1993**, *203*, 137−142.
(62) Cioslowski, J.; Stefanov, B. B. *Mol. Phys.* **1995**, *84*, 707−716.
(63) Stefanov, B. B.; Cioslowski, J. *J. Comput. Chem.* **1995**, *16*, 1394−1404.
(64) Pople, J. A. *Quart. Rev.* (*London*) **1957**, *11*, 273−290.
(65) Laing, M. *J. Chem. Educ.* **1987**, *64*, 124−128.
(66) Wiberg, K. B.; Marquez, M.; Castejon, H. *J. Org. Chem.* **1994**, *59*, 6817−6822.
(67) Macomber, R. *Organic Chemistry*; University Science Books: Susalito, CA, 1996; p 49.
(68) Jones, J. *Core Carbonyl Chemistry*; Oxford Science Publication: Oxford, UK, 1997; p 2.
(69) Brown, W. H.; Foote, C. S. *Organic Chemistry*, 2nd ed.; Saunders College Publishing: Fort Worth, TX, 1998; p 531.
(70) Brady, J. E.; Russell, J. W.; Holum, J. R. *Chemistry*: *The Study of Matter and Its Changes*, 3rd ed.; Wiley: New York, 2000; pp 400−401.
(71) Wheland, G. *Resonance in Organic Chemistry*; Wiley: New York, 1955; p 345.
(72) Pauling, L. *Nature of Chemical Bond*, 2nd ed.; Cornell University Press: Ithaca, NY, 1960; p 276.
(73) Wiberg, K. B.; Laidig, K. E. *J. Am. Chem. Soc.* **1987**, *109*, 5935−5943.
(74) Wiberg, K. B.; Breneman, C. M. *J. Am. Chem. Soc.* **1992**, *114*, 831−840.
(75) Wiberg, K. B.; Hadad, C. M.; Rablen, P. R.; Cioslowski, J. *J. Am. Chem. Soc.* **1992**, *114*, 8644−8654.
(76) Wiberg, K. B.; Rablen, P. R.; Rush, D. J.; Keith, T. A. *J. Am. Chem. Soc.* **1995**, *117*, 4261−4270.
(77) Wiberg, K. B. *J. Chem. Educ.* **1996**, *73*, 1089−1095.
(78) Wiberg, K. B. *Acc. Chem. Res.* **1999**, *32*, 922−929.
(79) Vassilev, N. G.; Dimitrov, V. S. *J. Mol. Struct.* **1999**, *484*, 39−47.

(80) Wiberg, K. B. *The Amide Linkage*: *Selected Structural Aspects in Chemistry, Biochemistry and Material Science*; Wiley: New York, 2000; pp 33−35.
(81) Wiberg, K. B.; Rush, D. J. *J. Org. Chem.* **2002**, *67*, 826−830.
(82) Laidig, K. E.; Cameron, L. M. *Can. J. Chem.* **1993**, *71*, 872−879.
(83) Kim, W.; Lee, H.-J.; Choi, Y. S.; Choi, J.-H.; Yoon, C.-J. *J. Chem. Soc., Faraday Trans.* **1998**, *94*, 2663−2668.
(84) Vassilev, N. G.; Dimitrov, V. S. *J. Mol. Struct.* **2000**, *522*, 37−46.
(85) Raos, G.; Bielli, P.; Tornaghi, E. *Int. J. Quantum Chem.* **1999**, *74*, 249−258.
(86) Bain, A. D.; Hazendonk, P.; Couture, P. *Can. J. Chem.* **1999**, *77*, 1340−1348.
(87) Wiberg, K. B.; Rablen, P. R. *J. Am. Chem. Soc.* **1995**, *117*, 2201−2209.
(88) Laidig, K. E.; Cameron, L. M. *J. Am. Chem. Soc.* **1996**, *118*, 1737−1742.
(89) Fogarasi, G.; Szalay, P. G. *J. Phys. Chem. A* **1997**, *101*, 1400−1408.
(90) Glendening, E. D.; Hrabal, J. A., II *J. Am. Chem. Soc.* **1997**, *119*, 12940−12946.
(91) Lauvergnat, D.; Hiberty, P. C. *J. Am. Chem. Soc.* **1997**, *119*, 9478−9482.
(92) Basch, H.; Hoz, S. *Chem. Phys. Lett.* **1998**, *294*, 117−125.
(93) Mo, Y.; Schleyer, P. v. R.; Wu, W.; Lin, M.; Zhang, Q.; Gao, J. *J. Phys. Chem. A* **2003**, *107*, 10011−10018.
(94) Quinonero, D.; Frontera, A.; Capo, M.; Ballester, P.; Suner, G. A.; Garau, C.; Deya, P. M. *New J. Chem.* **2001**, *25*, 259−261.
(95) Tsuchiya, S.; Seno, M. *J. Org. Chem.* **1979**, *44*, 2850−2855.
(96) Tsuchiya, S.; Seno, M.; Lwowski, W. *J. Chem. Soc., Chem. Commun.* **1982**, 875−876.
(97) Tsuchiya, S.; Seno, M.; Lwowski, W. *J. Chem. Soc., Perkin Trans. 2* **1983**, 887−890.
(98) Cameron, A. F.; Hair, N. J.; Morris, D. G.; Hawley, D. M. *J. Chem. Soc., Chem. Commun.* **1971**, 725−726.
(99) Cameron, A. F.; Hair, N. J.; Morris, D. G. *J. Chem. Soc., Perkin Trans. 2* **1972**, 1071−1076.
(100) Morris, D. G.; Muir, K. W.; Chii, C. O. W. *Polyhedron* **2003**, *22*, 3345−3353.
(101) Figueroa, J.; Racoveanu, A.; Gheorghiu, M. D.; Zakin, M. R. Manuscript in preparation.
(102) Swaminathan, S.; Craven, B. M.; McMullan, R. K. *Acta Crystallogr., Sect. B* **1984**, *B40*, 300−306.
(103) Zavodnik, V.; Stash, A.; Tsirelson, V.; De Vries, R.; Feil, D. *Acta Crystallogr., Sect. B* **1999**, *B55*, 45−54.
(104) Schultz, G.; Hargittai, I. *J. Phys. Chem.* **1993**, *97*, 4966−4969.
(105) Knapp, S.; Toby, B. H.; Sebastian, M.; Krogh-Jespersen, K.; Potenza, J. A. *J. Org. Chem.* **1981**, *46*, 2490−2497.
(106) Lumbroso, H.; Liegeois, C.; Morris, D. G.; Stephen, J. D. *Tetrahedron* **1978**, *34*, 557−562.
(107) Cioslowski, J.; Mixon, S. T.; Edwards, W. D. *J. Am. Chem. Soc.* **1991**, *113*, 1083−1085.
(108) Koch, U.; Popelier, P. L. A. *J. Phys. Chem.* **1995**, *99*, 9747−9754.
(109) Cannizzaro, C. E.; Houk, K. N. *J. Am. Chem. Soc.* **2002**, *124*, 7163−7169.
(110) Raymo, F. M.; Bartberger, M. D.; Houk, K. N.; Stoddart, J. F. *J. Am. Chem. Soc.* **2001**, *123*, 9264−9267.
(111) Taylor, R.; Kennard, O. *J. Am. Chem. Soc.* **1982**, *104*, 5063−5070.
(112) Glasstone, S. *Trans. Faraday Soc.* **1937**, *33*, 200−214.
(113) Donohue, J. In *Structural Chemistry and Molecular Biology*; Rich, A., Davison, N., Eds.; Freeman: San Francisco, CA, 1968; pp 459−463.
(114) Desiraju, G.; Steiner, T. *The Weak Hydrogen Bond*: *Applications to Structural Chemistry and Biology*; 1999.
(115) Steiner, T. *Chem. Commun.* (*Cambridge*) **1997**, 727−734.
(116) Steiner, T. *Cryst. Rev.* **1996**, *6*, 1−51.
(117) Desiraju, G. R. *Acc. Chem. Res.* **1996**, *29*, 441−449.
(118) Desiraju, G. R. *Acc. Chem. Res.* **1991**, *24*, 290−296.
(119) Sharon, A.; Maulik, P. R.; Vithana, C.; Ohashi, Y.; Ram, V. J. *Eur. J. Org. Chem.* **2004**, 886−893.
(120) Qin, X.-R.; Ishizuka, Y.; Lomas, J. S.; Tezuka, T.; Nakanishi, H. *Magn. Reson. Chem.* **2002**, *40*, 595−598.
(121) Gatti, C.; May, E.; Destro, R.; Cargnoni, F. *J. Phys. Chem. A* **2002**, *106*, 2707−2720.
(122) Nagawa, Y.; Yamagaki, T.; Nakanishi, H.; Nakagawa, M.; Tezuka, T. *Tetrahedron Lett.* **1998**, *39*, 1393−1396.
(123) Sarkhel, S.; Desiraju, G. R. *Proteins*: *Struct., Funct., Bioinformatics* **2003**, *54*, 247−259.
(124) Vargas, R.; Garza, J.; Dixon, D. A.; Hay, B. P. *J. Am. Chem. Soc.* **2000**, *122*, 4750−4755.
(125) Rogers, M. T.; Woodbrey, J. C. *J. Phys. Chem.* **1962**, *66*, 540−544.
(126) Rabinovitz, M.; Pines, A. *J. Am. Chem. Soc.* **1969**, *91*, 1585−1589.
(127) Ross, B. D.; Wong, L. T.; True, N. S. *J. Phys. Chem.* **1985**, *89*, 836−839.
(128) Wawzonek, S. *Ind. Eng. Chem. Prod. Res. Dev.* **1980**, *19*, 338−349.
(129) Timpe, H. J. *Z. Chem.* **1972**, *12*, 250−261.
(130) McKillip, W. J.; Sedor, E. A.; Culbertson, B. M.; Wawzonek, S. *Chem. Rev.* **1973**, *73*, 255−281.
(131) Greenberg, A.; Venanzi, C. A. *J. Am. Chem. Soc.* **1993**, *115*, 6951−6957.
(132) Greenberg, A.; Moore, D. T.; DuBois, T. D. *J. Am. Chem. Soc.* **1996**, *118*, 8658−8668.